

# RF Output Signal Commutation in Multi-channel Electrosurgical Unit

Kiril Ivanov\*, Ivo Iliev

Department of Electronics  
Technical University of Sofia  
8 Kliment Ohridski Blvd., Sofia 1000, Bulgaria  
E-mails: [kiril.sl.ivanov@gmail.com](mailto:kiril.sl.ivanov@gmail.com), [izi@tu-sofia.bg](mailto:izi@tu-sofia.bg)

\*Corresponding author

Received: April 11, 2019

Accepted: February 28, 2020

Published: June 30, 2020

**Abstract:** This article reviews the existing problems with the output power commutation in electrosurgical units (ESU) in cases of multi-channel configuration, with requirement for high speed commutation rate between connectors, including in active mode. Attention is drawn to the methods for transmitting the output power to different outputs. A new type of output signal management based on the use of magnetic amplifiers is proposed. The proposed hardware solution is preliminary simulated and tested with PSpice A/D (Cadence product). The achieved results are analyzed and commented. Tests also are performed with physically realized device and the results are analyzed and evaluated in context of applicability in multi-channel ESU as well as in sterilization equipment.

**Keywords:** RF output control, Electrosurgery, ESU, Magnetic amplifier (MAG AMP).

## Introduction

Commutation of the output power is a critical part in the electrosurgical units (ESU), especially in cases with more than 4 outputs. The specificity of the problem relates to the requirement to guarantee enough insulation between the output stage and the output connectors. Therefore, the Radio Frequency (RF) current/voltage commutation module is an important part of this type of medical devices. The RF output current can be applied to the tissues in two main configurations – monopolar and bipolar. In the monopolar configuration, the RF current is flowing from the active electrode thru the body of the patient to the dispersive electrode. Most important are the contact areas of the monopolar active electrode and the dispersive electrode. The bigger the contact area is the lower is the current density thus reducing the heating of the tissue. In the monopolar mode, the active and dispersive electrodes should be close to each other, so the current is flowing only thru the tissue that is treated. In bipolar mode, the contact area of the active and return electrodes are the same, so the heating of the tissue is the same. Besides the type of application on the RF power on the tissue, the signal itself creates different effects on the treated areas.

The RF current in the electrosurgery is one of the most critical components of the ESU. Different current waveforms have a different effect on the treated tissue and are represented as different modes of operation. Most common monopolar modes are – Cut mode, Blend mode, Pinpoint mode and Spray mode. Each of these modes has different waveform of the signal and different parameters – maximum Root Mean Square (RMS) current, maximum RMS voltage, maximum peak voltage, etc. For example, Cut mode waveform is a continuous wave with high RMS current and relatively low RMS voltage. These characteristics of the mode are ideal for cutting the tissue with minimum lateral damage. The high RMS value of the current is creating

a lot of heat in the tissue cells. The lack of OFF periods in the waveform (continuous wave) is not allowing the treated tissue to cool down. Because of the high RMS current and the continuous waveform, the water inside the cells is rapidly heated and rapidly evaporated. This is creating the cutting effect. If the current is modulated (with ON and OFF periods) the cutting effect will be reduced, and the lateral damage will increase. This has another benefit – coagulating the tissues, thereby reducing/stopping the bleeding. Also, with the increasing of the OFF time, the peak voltage increases too, allowing better coagulation.

One more monopolar mode that is not common for all ESU manufacturers is the plasma mode. Plasma is an ionized gas consisting of positive ions and free electrons in proportions resulting in more or less no overall electric charge, typically at low pressures (as the upper atmosphere and in fluorescent lamps) or at very high temperatures (as in stars and nuclear fusion reactors). Some ESU manufacturers create artificial plasma by applying a very high voltage (more than 4 kV peak) in a gas-saturated area (most common are helium or argon). This plasma has some advantages in comparison to the common modes – better coagulation and ablation and reduced tissue carbonization due to the lack of oxygen in the treated area. As for the common monopolar modes, the waveform of the RF current affects the end effect on the treated tissue as described above.

All the signal parameters need to be taken into consideration when designing a commutation module for an ESU.

The system architecture of the commutation module (Fig. 1) is composed of the following blocks: RF output block, Digital control block, Isolation block, Switching block, and  $R_{LOAD}$ , where:

- RF output – the output stage of ESU;
- Digital control – generates driving signals for the switching block with frequencies getting up to 100 Hz;
- Isolation – provides separation between the digital control block and the switching block which guarantees shielding against influence of the RF voltages with high intensity;
- Commutation – the commutation block (ON/OFF) drives the contact between the RF output and the loads. This block also must provide insulation between the RF output and the different connectors – reducing the risk of RF voltage being present at a wrong output connector;
- $R_{LOAD}$  – output load, simulates the patient's body during treatment.

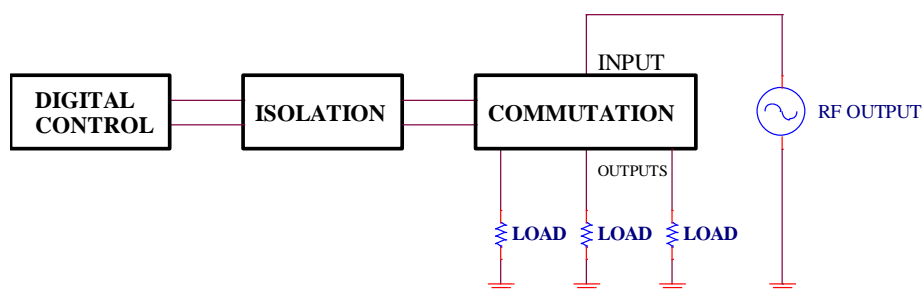


Fig. 1 Commutation module block diagram

The most common circuit solution of the commutation module is based on the use of relays as key elements. These relays shall be capable of withstanding higher than the maximum peak voltages in any of the ESU modes. For example, in Spray mode, the output peak voltage in

some ESUs is up to 4 kV [5, 8, 13]. Prevalingly used are the reed relays (gas capsule with inert gas in it) providing insulation between the terminals up to 5 kV. Advantages of the reed relays are the low price and high reliability. Disadvantages are low commutation speed and disability to switch the output when the RF output stage is active [1, 6]. Actually, the commutation is possible during active output, but will result in sparks creation and carbonization on the reed surface. This carbonization increases the impedance of the contacts and significantly reduce the life cycle of the ESU.

### *Magnetic amplifier as an alternative of relays in commutation module*

The magnetic amplifier (also known as “MAG AMP”) is an electromagnetic device that amplifies electrical signals [4]. Visually a MAG AMP device may resemble a transformer, but the operating principle is quite different – essentially the MAG AMP is a saturable reactor (Fig. 2). It makes use of magnetic saturation of the core, a non-linear property intrinsic of a certain class of transformer cores [12]. For controlled saturation characteristics, the magnetic amplifier employs core materials with specific magnetization curve shape that is highly rectangular, in contrast to the slowly tapering curve of softly saturating core materials, often used in conventional transformers [1, 4, 9-12, 14].

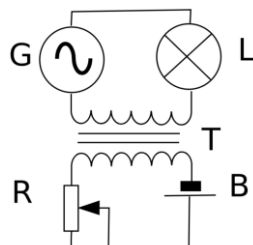


Fig. 2 Saturable reactor, illustrating the principle of a magnetic amplifier

The typical magnetic amplifier consists of two physically separated, but similar transformer magnetic cores, each of which has two windings: a control winding and an AC winding. A small DC current from a low-impedance source is fed into the series-connected control windings [4, 11]. The AC windings can be connected either in series or in parallel, configurations which determine the different types of MAG AMPs. The amplitude of the control current flowing through the control winding sets the point of the core saturation [2, 3]. In saturated state, the AC winding will go from high-impedance state (“OFF”) into a very low-impedance state (“ON”) [1, 4, 9-12, 14]. A relatively small DC current on the control winding can control (switch) large AC currents through the AC windings. This leads to current amplification [10].

Two magnetic cores are used because the AC current will generate a high voltage in the control windings. By connecting them in opposite phase, the two cancel each other, so that no current is induced in the control circuit [12, 14].

The functional characteristics of the magnetic amplifier make it an appropriate choice for realization or composition of the ESU commutation block. It allows to start and stop the RF output current/voltage, at high repetition rates during an active procedure.

In the focus of this paper are experimental investigations, simulations, and parametric analyses, associated with multi-channel ECU switching block, realized by a magnetic amplifier.

## Materials and methods

The schematic corresponding to the block diagram on Fig. 1 was simulated on PSpice A/D (Cadence product). Isolation block is built with an optocoupler. Design of the switching circuit (commutation) is based on the magnetic amplifier schematic described above. A toroidal ferrite core is used – Ferroxcube TX/51/32/19, 3F36 material. This material is selected because of its complex permeability (Fig. 3) as a function of the frequency characteristics.

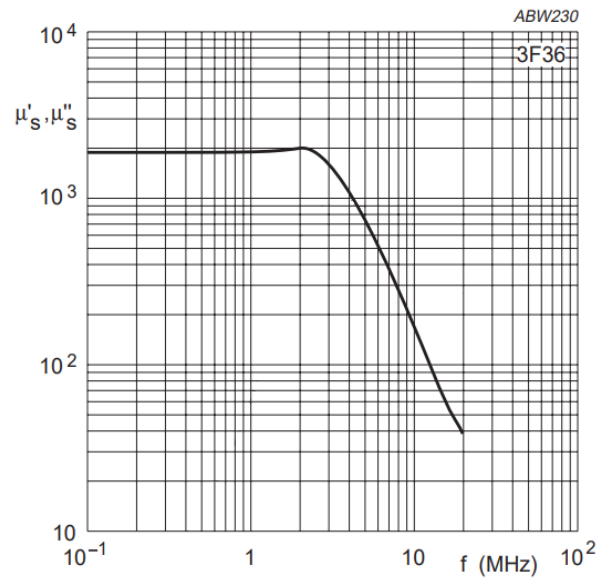


Fig. 3 Complex permeability as a function of frequency

The complex permeability of the 3F36 material is constant up to 2 MHz. The selected frequency of an RF source is 450 kHz and the amplitude is  $V_{P-P} = 2000$  V. The load is simulated by a  $1000 \Omega$  resistor. This value was selected experimentally [7].

Fig. 4 shows the output voltage before and after the MAG AMP in “ON” state. With red is shown the voltage at the RF generator output (before the MAG AMP) and with black – the voltage after the MAG AMP (at the load).

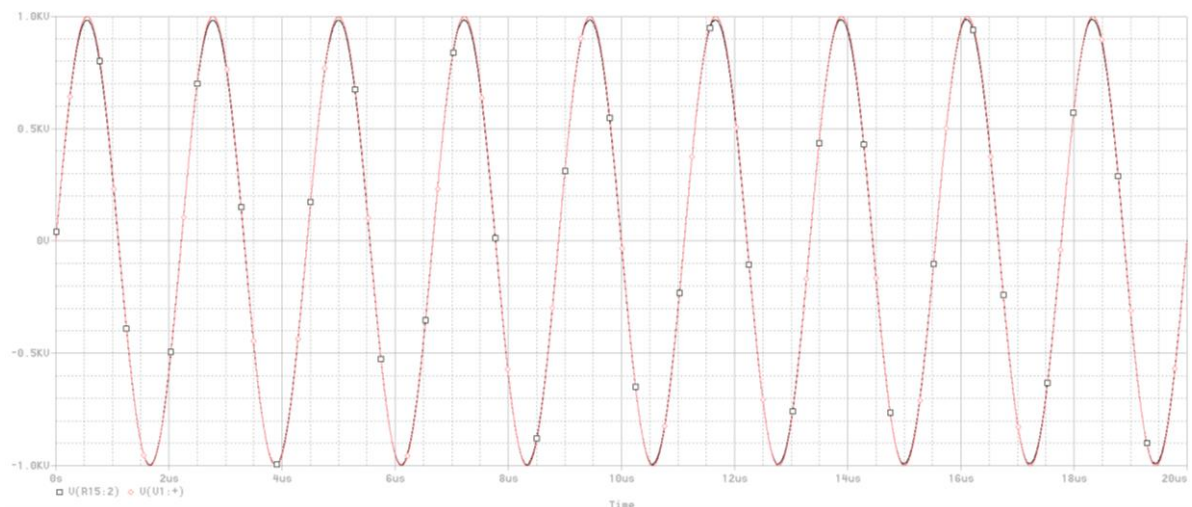


Fig. 4 Simulation results in MAG AMP “ON” state

In this amplitude scale, both voltages almost completely coincide. The small peak difference (less than 37 V) is due to the leakage impedance of the transformer. In the simulation, the leakage inductance is set to 4% of the inductances of the AC and the control windings.

Fig. 5 shows the output voltage before and after the MAG AMP in “OFF” state. With red is shown the voltage at the RF generator output (before the MAG AMP) and with black – the voltage after the MAG AMP (on the load).

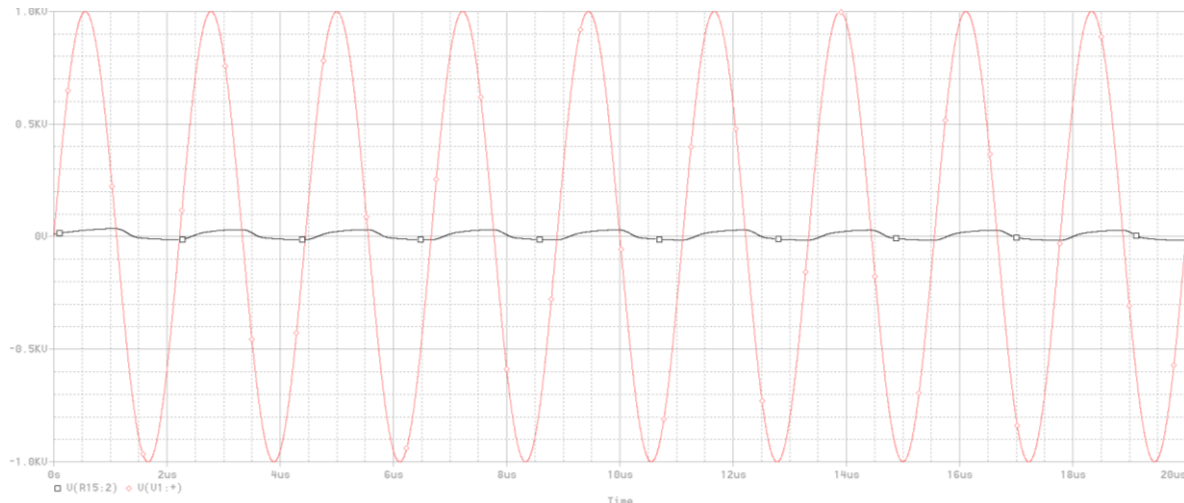


Fig. 5 Simulation results in MAG AMP “OFF” state

The output voltage has a very low peak voltage ( $\approx 26$  V) and considerably changed waveform. This low voltage does not allow plasma ignition when load is present at the output, otherwise bursts of plasma may be present. This needs to be investigated furthermore. These parameters confirm the possibility of realizing a multi-channel plasma generation system with or allowing individual control of MAG AMPs at every channel.

## Experimental results

A test module for experimental investigations was realized considering the simulation results. All tests are performed using standard ESU with embedded plasma generation module. Output power is measured at three different modes – CUT mode, J-Plasma with an external transformer (Active J-Plasma mode) and J-Plasma with an internal transformer (Passive J-Plasma mode). CUT mode is a standard electrosurgical mode, the J-Plasma mode with an external transformer is a current generator, and the J-Plasma mode with an internal transformer is a high impedance electrosurgical mode. Three different MAG AMP structures are tested and evaluated.

Output power curves of the selected modes are given in the Fig. 6-8. Load impedances differ because of the specificities of each of the selected modes. For example, the CUT mode power curve is up to  $2000 \Omega$  since this is the maximum expected tissue impedance for this mode.

As noted above the selected ferrite material for the tests is 3F36 (TX/51/32/19). The inductance factor ( $A_L$ ) of this material is  $\sim 2400$  nH. Based on this value as well as on the results from the simulation, the selected turns for the Primary (AC) and Secondary (control) windings are respectively 54 and 27.

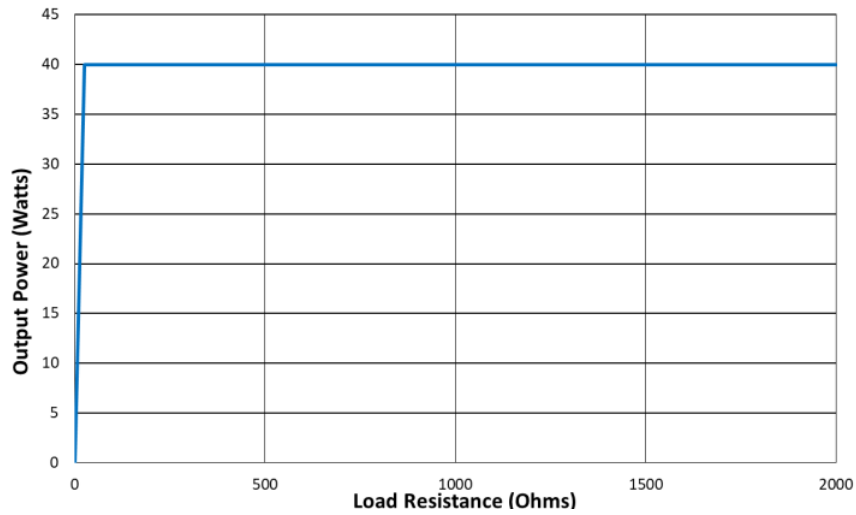


Fig. 6 Output power curve in CUT mode (40 W power set)

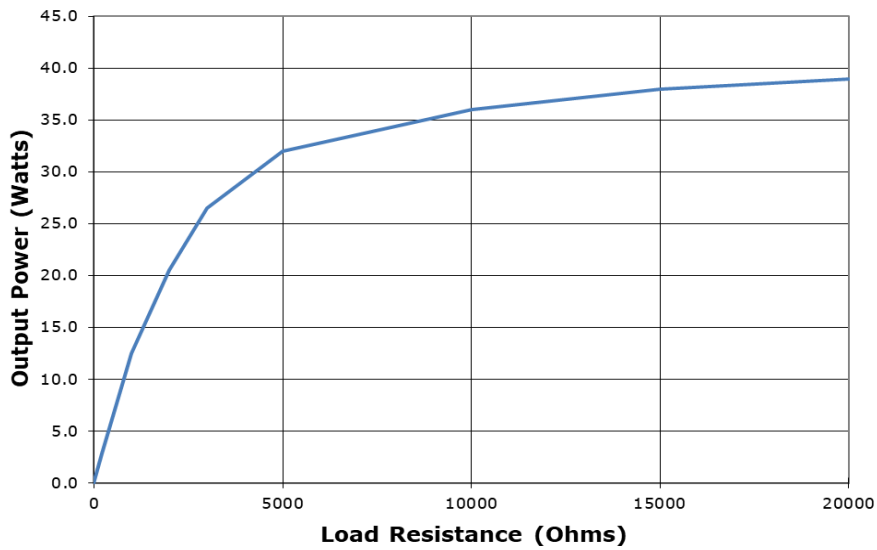


Fig. 7 Output power curve in J-Plasma mode with external STEP UP transformer (100% power set)

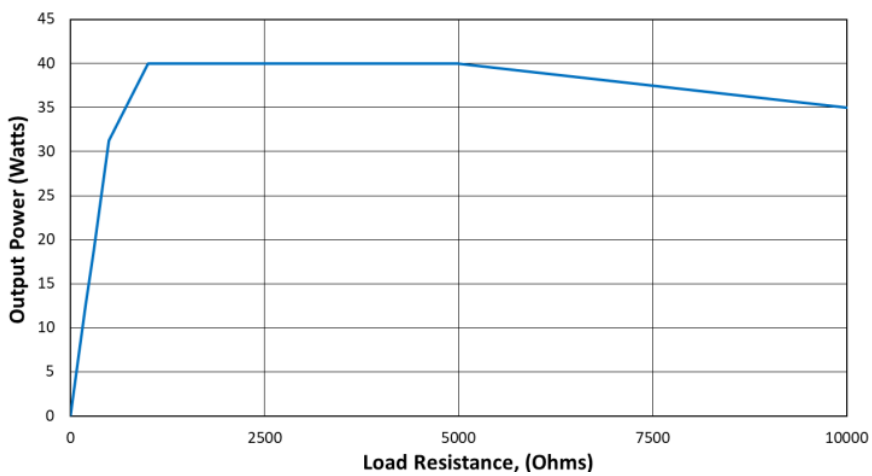


Fig. 8 Output power curve in J-Plasma mode with internal STEP-UP transformer (100% power set)

AWG 28 wire is used for the windings (Fig. 9). It has enough permeability for the output current corresponding to the selected modes.

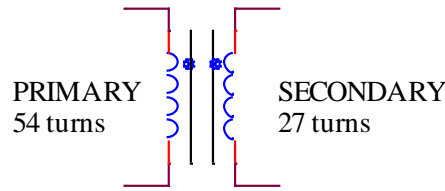


Fig. 9 MAG AMP structure – windings and turns

The measured constructive parameters of each MAG AMP before the tests are: (i) the inductance of the AC and Control windings ( $L_{AC}$  and  $L_{CTRL}$ ); (ii) the leakage inductance of the AC and Control windings ( $L_{AC_{LEAK}}$  and  $L_{CTRL_{LEAK}}$ ); (iii) the capacitance between the two windings (see Table 1). Leakage inductances and the capacitance between the windings are affected mostly by the MAG AMP structure. A comparison between the parameters of the MAG AMPs and the test results are done to evaluate the different proposed constructions. All measurements are performed at frequency – 100 kHz, and are given in Table 1.

Table 1. Different MAG AMP structures and their parameters

	Structure 1	Structure 2	Structure 3
<b>AC winding</b>	Directly over the ferrite Turns as close as possible		Directly over the ferrite. Turns evenly placed on the full surface of the ferrite.
<b>Insulation</b>	PTFE isolation 0.2 mm 50% overlapping		
<b>Control winding</b>	Directly over the PTFE Centered over the AC winding	Directly over the PTFE Evenly placed over the AC winding	
<b><math>L_{AC}</math>, mH</b>	6.85	6.7	6.6
<b><math>L_{AC_{LEAK}}</math>, <math>\mu</math>H</b>	37.8	11.6	14.0
<b><math>L_{CTRL}</math>, mH</b>	1.73	1.67	1.65
<b><math>L_{CTRL_{LEAK}}</math>, <math>\mu</math>H</b>	9.7	3.0	3.7
<b>C, pF</b>	29.4	35.9	42.1

Test results are presented below with column bars for clarity.

### Voltage measurements

#### CUT mode – 40 W power setting

The graphics on Fig. 10 and Fig. 11 demonstrate that in a CUT mode the  $V_{P-P}$  is strongly affected by the capacitance between the windings and the leakage inductance. In “ON” state the higher the capacitance the lower the voltage. In the “OFF” state, the output voltage depends on the load impedance. The lower the load impedance, the lower is the output voltage (peak-to-peak). The results in case “NO LOAD” are indicative on the influence of the used measurement equipment – oscilloscope with input impedance 100 M $\Omega$  and capacitance 3 pF.

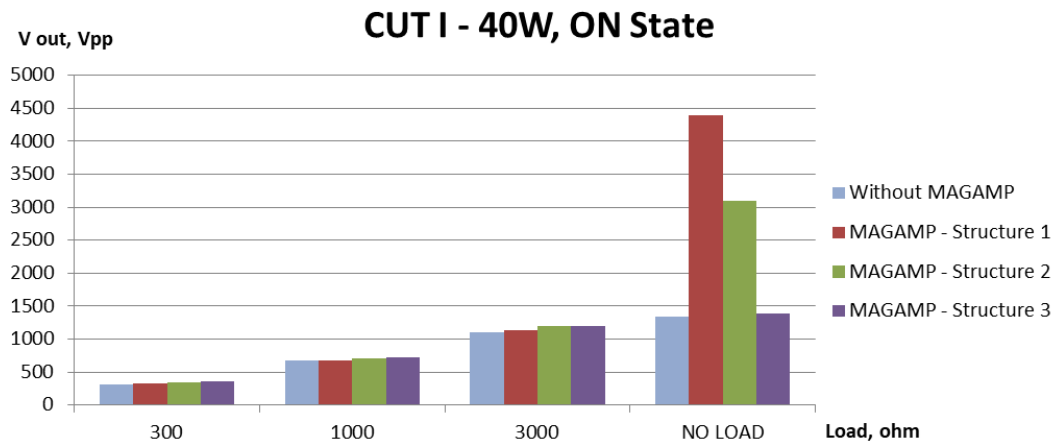


Fig. 10 MAG AMP structures in “ON” state – CUT mode 40 W power setting (peak-to-peak voltage)

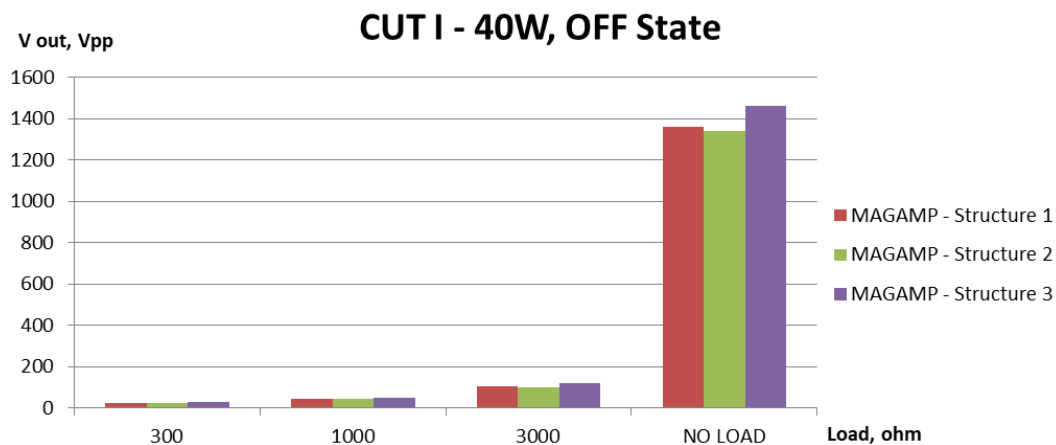


Fig. 11 MAG AMP structures in “OFF” state – CUT mode 40 W power setting (peak-to-peak voltage)

#### *Active J-Plasma mode – 100% power setting*

The graphics on Fig. 12 and Fig. 13 demonstrate that in Active J-Plasma mode the  $V_{P,P}$  is strongly affected by the capacitance between the windings and the leakage inductance. In “ON” state the lower the leakage inductance, the higher the voltage. This is correct no matter the load at the output. In the “OFF” state, the output voltage depends on the leakage inductance. The lower the leakage inductance, the lower is the output voltage (peak-to-peak). When there is no load at the output, the voltage depends more on the capacitance between the AC and the control windings. This, however, needs to be investigated more.

#### *Passive J-Plasma mode – 100% power setting*

The graphics on Fig. 14 and Fig. 15 demonstrate that in Passive J-Plasma mode the  $V_{P,P}$  is strongly affected by the capacitance between the windings and the leakage inductance. In “ON” state the lower the leakage inductance, the higher the voltage. This is correct when the output is loaded. When there is no load, more representative is the capacitance between the windings. The lower the capacitance, the higher is the output voltage. In the “OFF” state, the output voltage depends on the capacitance between the windings. The higher the capacitance, the higher is the output voltage (peak-to-peak).



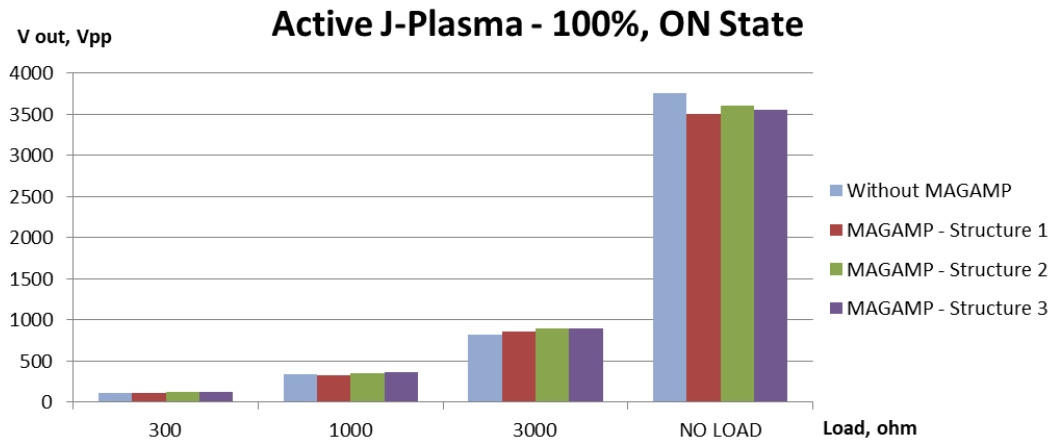


Fig. 12 MAG AMP structures in “ON” state – Active J-Plasma mode 100% power setting (peak-to-peak voltage)

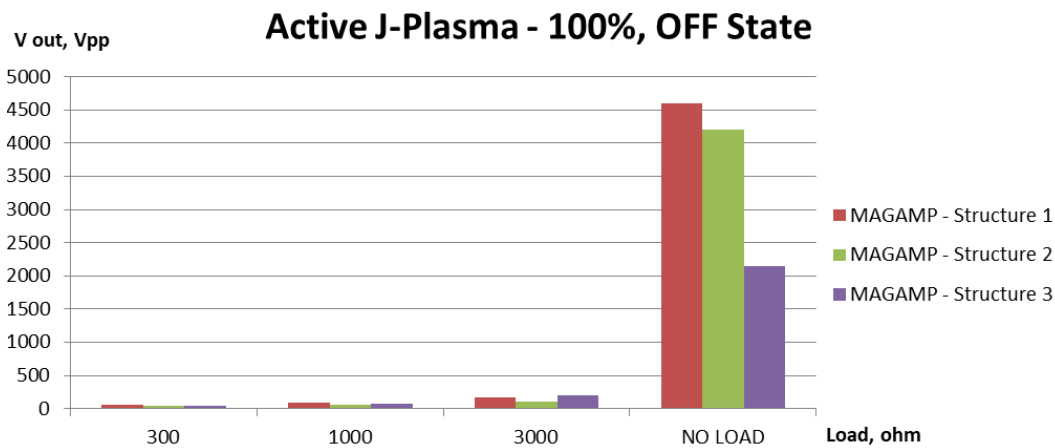


Fig. 13 MAG AMP structures in “OFF” state – Active J-Plasma mode 100% power setting (peak-to-peak voltage)

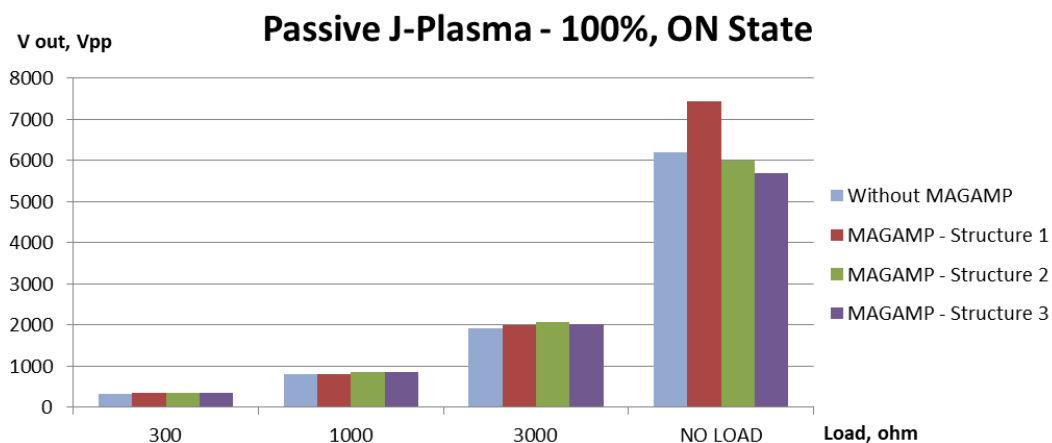


Fig. 14 MAG AMP structures in “ON” state – Passive J-Plasma mode 100% power setting (peak-to-peak voltage)

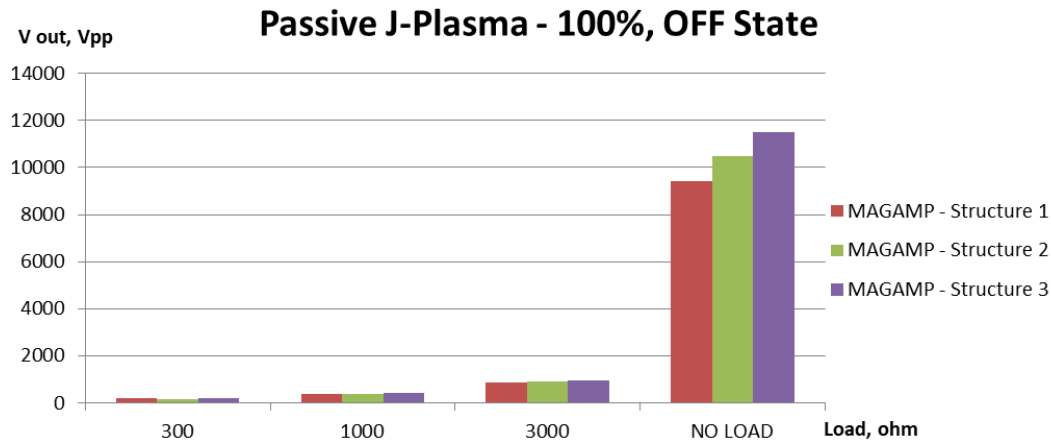


Fig. 15 MAG AMP structures in “OFF” state – Passive J-Plasma mode 100% power setting (peak-to-peak voltage)

### Current measurements

#### CUT mode – 40 W power setting

The graphics on Fig. 16 and Fig. 17 demonstrate that in CUT mode the output current is strongly affected by the leakage inductance of the windings. In “ON” state the lower the leakage inductance the higher is the output current. In “OFF” state lower leakage inductance is resulting in lower output current.

#### Active J-Plasma mode – 100% power setting

The graphics on Fig. 18 and Fig. 19 demonstrate that in Active J-Plasma mode the output current is strongly affected by the leakage inductance of the windings. In “ON” state the lower the leakage inductance the higher is the output current. In “OFF” state higher capacitance between the windings is resulting in lower output current.

#### Passive J-Plasma mode – 100% power setting

The graphics on Fig. 20 and Fig. 21 demonstrate that in Passive J-Plasma mode the output current is strongly affected by the capacitance between the windings. In “ON” state the lower the capacitance the higher is the output current. In “OFF” state higher capacitance between the windings is resulting in lower output current.

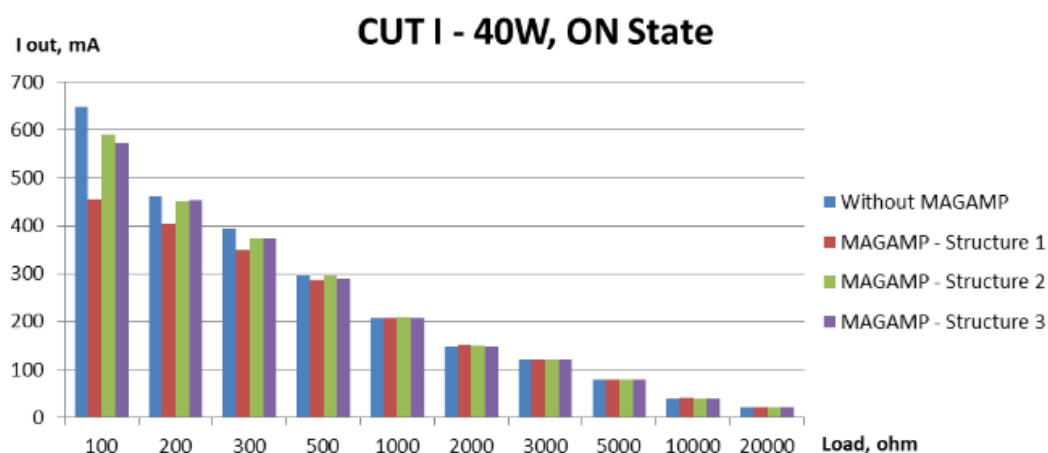


Fig. 16 MAG AMP structures in “ON” state – CUT mode 40 W power setting

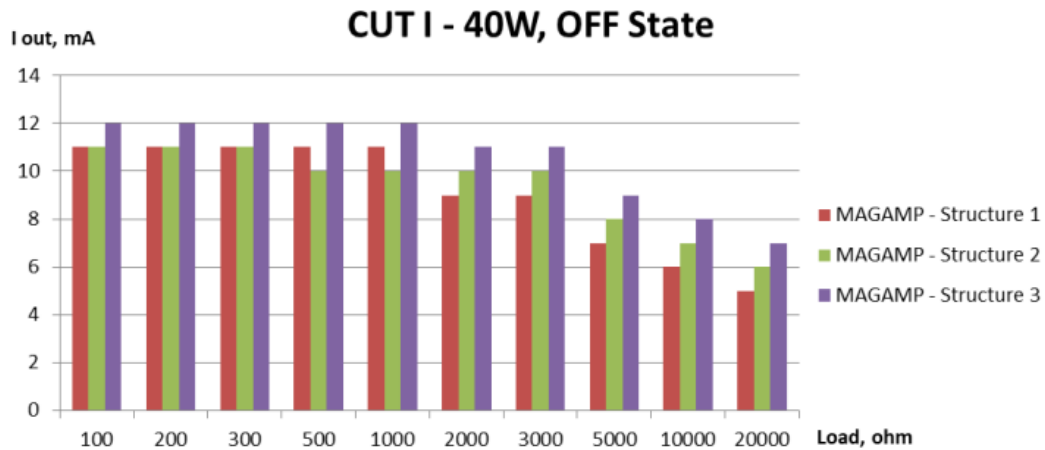


Fig. 17 MAG AMP structures in “OFF” state – CUT mode 40 W power setting

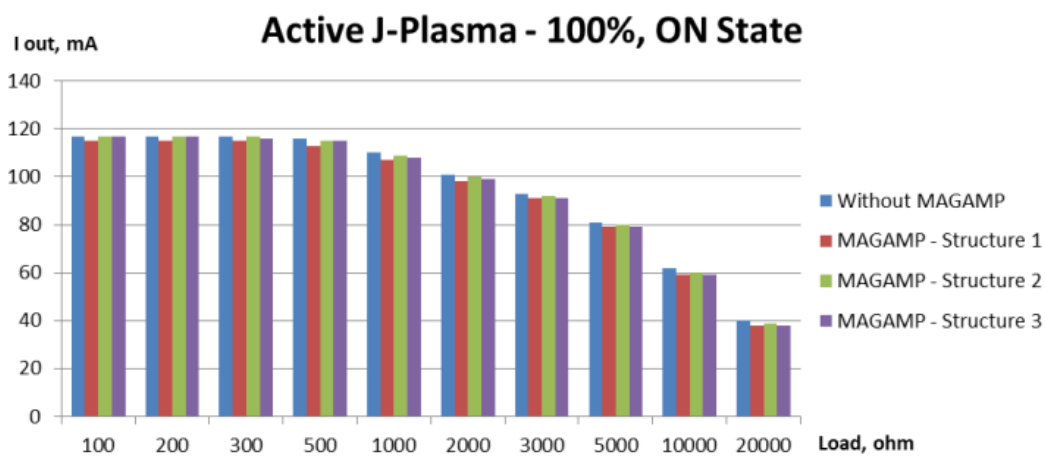


Fig. 18 MAG AMP structures in “ON” state – J-Plasma mode with external transformer 100% power setting

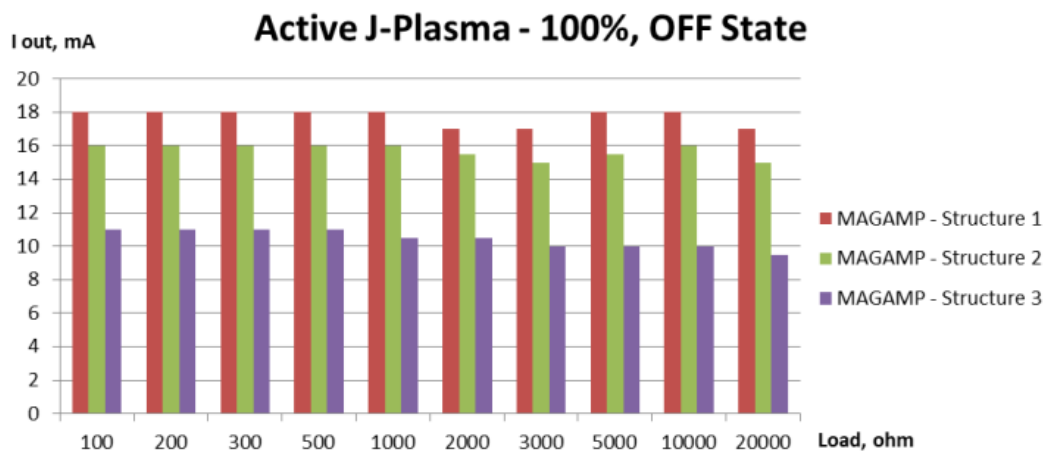


Fig. 19 MAG AMP structures in “OFF” state – J-Plasma mode with external transformer 100% power setting

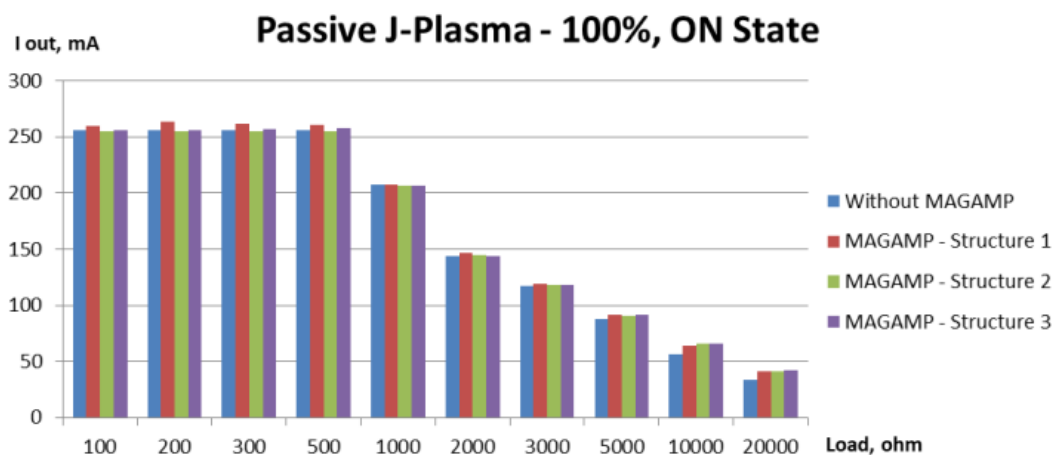


Fig. 20 MAG AMP structures in “ON” state – J-Plasma mode with internal transformer 100% power setting

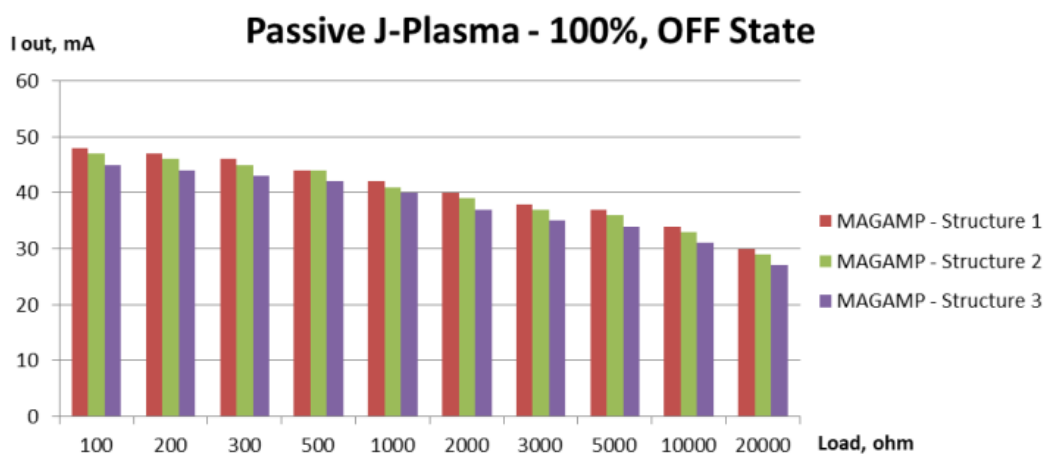


Fig. 21 MAG AMP structures in “OFF” state – J-Plasma mode with internal transformer 100% power setting

*Overall evaluation of test results*

The graphics on Fig. 10 to Fig. 15 demonstrate that the  $V_{P-P}$  is strongly affected by the leakage inductance and the capacitance between the windings. Different modes react differently. This effect creates an inconsistency with the structures with higher capacitance. Another observed effect is the reduction of the output current in dependence on the leakage inductance of the MAG AMP. Lower leakage inductance results in lower output current in the “OFF” state. However, this effect also depends on the output power mode.

**Conclusion**

The functional characteristics of MAG AMPs in a great deal answer to the requirements defined to the commutation module in multi-channel ESU. Besides the possibilities for commutation of high voltages, additional benefit is the switching speed between the different outputs (tools). Such speed is not achievable with the relays commonly used in the most electrosurgical units. The test results showed that the most balanced MAG AMP-based switching solution is the structure with parameters:

- AC winding directly over the ferrite with turns as close as possible;
- PTFE isolation 0.2 mm with 50% overlapping;

- The control winding directly over the PTFE with turns evenly placed over the AC winding.

The proposed conception can extend the applicability of multi-channel plasma generators in areas as plasma sterilization, decontamination of foods and liquids, etc.

A negative effect observed during the tests is the increase in the peak-to-peak voltage in the “OFF” state when no load is connected to the output of the unit. The hypothesis is that this could be caused by resonance between the RF output stage and the MAG AMP. This effect and its impact should be in-deep investigated and considered in future developments of the designed module.

## Acknowledgements

*This study is supported by the Bulgarian National Scientific Fund, Grant DN 07/21.*

## References

1. Ahamed S. V., V. B. Lawrence (1997). Design and Engineering of Intelligent Communication Systems, Springer Science & Business Media, New York.
2. Austrin L. (2007). On Magnetic Amplifiers in Aircraft Applications, KTH, School of Electrical Engineering (EES), Electromagnetic Engineering, Licentiate Thesis, Stockholm.
3. Boeke U. (2005). Scalable Fluorescent Lamp Driver Using Magnetic Amplifiers, European Conference on Power Electronics and Applications, 10.1109/EPE.2005.219246.
4. Gilmore K. (1960). Magnetic Amplifiers – How They Work and What They Do, Popular Electronics, 13(1), 71-75.
5. Halliday D., R. Resnick, J. Walker (2007). Fundamentals of Physics, 8<sup>th</sup> Ed., John Wiley & Sons, Inc., Hoboken, New York.
6. <https://www.pickeringrelay.com/>, How Do Reed Relays Compare with Other Switching Technologies? (Last access 26 June 2020).
7. Ivanov K., I. Iliev, S. Tabakov (2018). Plasma-based Sterilization Using New Multipoint Ignition Accessory, E+E, 53, 10-15.
8. Kalkwarf K. L., R. F. Krejci, A. R. Edison (1979). A Method to Measure Operating Variables in Electrosurgery, J Prosthet Dent, 566-570.
9. Kemp B. (1962). Magnetic Amplifiers. Fundamentals of Magnetic Amplifiers, Howard W. Sams & Co., Indianapolis, USA.
10. Mali P. (1960). Magnetic Amplifiers – Principles and Applications, A Rider Publication, No. 261, J. F. Rider, The Ohio State University, USA.
11. Pressman A. I. (1997). Switching Power Supply Design, McGraw-Hill.
12. Storm H. F. (1955). Magnetic Amplifiers, John Wiley & Sons, Inc., New York.
13. Swerdlow D. B., E. P. Salvati, R. J. Rubin, S. B. Labow (1974). Electrosurgery: Principles and Use, Dis Colon Rectum, 17(4), 482-486, doi: 10.1007/BF02587025.
14. Westman H. P., M. M. Perugini, M. Karsh, et al. (Eds.) (1968). Reference Data for Radio Engineers, 5<sup>th</sup> Ed., Howard W. Sams & Co., Div. ITT.

**Kiril Ivanov, Ph.D. Student**E-mail: [kiril.sl.ivanov@gmail.com](mailto:kiril.sl.ivanov@gmail.com)

Kiril Ivanov obtained his M.Sc. degree (2014) from the Faculty of Telecommunications, Technical University of Sofia. Currently he is a Ph.D. Student at the Department of Electronics, Technical University of Sofia. Kiril Ivanov's interests are mainly in design and development of electrosurgical apparatus and different methods for decontamination and sterilization.

**Prof. Ivo Iliev, Ph.D., D.Sc.**E-mail: [izi@tu-sofia.bg](mailto:izi@tu-sofia.bg)

Ivo Iliev obtained his M.Sc. degree from the Faculty of Electronic Engineering and Technologies, Technical University of Sofia. His Ph.D. thesis was on the new methods and approaches applicable in holters for blood pressure measurement. In 2010 he obtained the Dr.Eng.Sci. degree on Patient Telemetry. Since 2013, he has been a Professor in Biomedical Engineering. Currently he is a Dean of the Faculty of Electronic Engineering. His interests are mainly in the field of acquisition, pre-processing, analysis and recording of biomedical signals, patient telemetry, and assistive systems for elderly.



© 2020 by the authors. Licensee Institute of Biophysics and Biomedical Engineering, Bulgarian Academy of Sciences. This article is an open access article distributed under the terms and conditions of the Creative Commons Attribution (CC BY) license (<http://creativecommons.org/licenses/by/4.0/>).